Toxicologic Pathology, 39: 22-35, 2011

ISSN: 0192-6233 print / 1533-1601 online
DOI: 10.1177/0192623310389621

Histology of the Central Nervous System

Robert H. Garman

Consultants in Veterinary Pathology, Inc., Murrysville, Pennsylvania, USA

Abstract

The intent of this article is to assist pathologists inexperienced in examining central nervous system (CNS) sections to recognize normal and abnormal cell types as well as some common artifacts. Dark neurons are the most common histologic artifact but, with experience, can readily be distinguished from degenerating (eosinophilic) neurons. Neuron degeneration stains can be useful in lowering the threshold for detecting neuron degeneration as well as for revealing degeneration within populations of neurons that are too small to show the associated eosinophilic cytoplasmic alteration within H&E-stained sections. Neuron degeneration may also be identified by the presence of associated macroglial and microglial reactions. Knowledge of the distribution of astrocyte cytoplasmic processes is helpful in determining that certain patterns of treatment-related neuropil vacuolation (as well as some artifacts) represent swelling of these processes. On the other hand, vacuoles with different distribution patterns may represent alterations of the myelin sheath. Because brains are typically undersampled for microscopic evaluation, many pathologists are unfamiliar with the circumventricuar organs (CVOs) that represent normal brain structures but are often mistaken for lesions. Therefore, the six CVOs found in the brain are also illustrated in this article.

Keywords: astrocyte; circumventricular organs; microglia; neuron; dark neuron; neuron degeneration stains; oligodendrocyte.

Introduction

This article represents a mini-atlas that displays the normal and altered morphologic features of neurons, macroglia, and microglia within the CNS, as well as classic patterns of cell degeneration and artifact. Images of the circumventricular organs are also included, because this author has found some of these normal structures to be misinterpreted as lesions.

The CNS is composed of hundreds of diverse neuroanatomic regions (many referred to as "nuclei") and is frequently undersampled microscopically. It is important for pathologists to appreciate this diversity, to become familiar with rudimentary neuroanatomic landmarks, and to have an appreciation of the differential sensitivities of these varying brain regions to excitotoxicity as well as to physical and/or chemical insult. Some knowledge of neurochemistry, as well as of the afferent and efferent connections of individual brain nuclei, is helpful. At the very least, lesions that are detected should be identified as to specific neuroanatomic location, and regions receiving afferents from the affected region (or projecting to it) should also be examined microscopically. To interpret cytologic alterations, it is important for the pathologist to recognize both normal and pathologic variations in the appearances of the cells residing within the CNS. The pathologist must also have knowledge of histologic artifacts that are common within sections of the CNS, because these artifacts may be misinterpreted as lesions or may potentially mask underlying neuropathologic processes. With experience, recognition of artifacts should not present a problem for the pathologist even if the tissues are not optimally handled.

Because the information presented in this article is relatively basic, only selected references are included. There are many excellent neuropathology texts that present greater detail (and many more images), and these titles can be found in the extensive bibliography presented by Bolon et al. (2011).

Cells of the central nervous system are typically divided into the following two major categories:

I. Cells of neuroectodermal origin
   - Neurons
   - Astrocytes
   - Oligodendrocytes
   - Ependymocytes

II. Cells of mesenchymal origin
   - Meninges
   - Blood vessels
   - Adipose tissue
   - Microglia

The images and discussion in this article are limited to neurons, astrocytes, oligodendrocytes and microglia. Images of the circumventricular organs are also included.

Neurons

As one measure of brain complexity, it is generally stated that there are approximately 100 billion neurons in the human

Address correspondence to: Robert H. Garman, DVM, Consultants in Veterinary Pathology, Inc., PO Box 68, Murrysville, PA 15668-0068; e-mail: vetpathol@cs.com.

Abbreviations: CD68 (ED1), a glycoprotein expressed predominantly on lysosomal membranes of myeloid cells (including tissue macrophages); CNS, central nervous system; CVO, circumventricular organ; GABA, γ-amino butyric acid (the principal inhibitory neurotransmitter in the brain); GFAP, glial fibrillary acidic protein (a marker for astrocytes); $GSIB_4$, *Griffonia simplicifolia*-IB4 (a stain for microglia); H&E, hematoxylin and eosin; Iba1, ionized calcium-binding adapter molecule 1 (a marker for microglial cells); MAG, myelin-associated glycoprotein; MAP2, microtubule associated protein 2; MBP, myelin basic protein; NeuN, an immunostain for "Neuronal Nuclei"; RER, rough endoplasmic reticulum.

brain and even greater numbers of glial cells. Neurons are characterized by wide variations in size as well as shape (especially when special stains are used to reveal their cytoplasmic processes). Neurons may be broadly classified as ''small neurons'' or ''large neurons,'' but anatomic subtypes of each of these categories exist. Neurons may also be classified according to the neurotransmitters that they release (e.g., cholinergic, glutamatergic, GABAergic). Most neurons have multiple dendrites arising from their cell bodies. However, with rare exceptions, each neuron has only a single axon (even though this axon may branch at points distal to its cell body). Axons are specialized for transport, for the conduction of waves of depolarization, and for synaptic transmission. The Nissl substance, which stains quite prominently in large-sized neurons but is usually not apparent in small-sized neurons at the light microscopic level, represents the rough endoplasmic reticulum (RER) (best seen in Figure 1a). The RER is primarily confined to the neuronal soma but may penetrate slightly into the axonal hillock. The axon contains large numbers of neurofilaments and microtubules. These structural elements are important for maintaining cell integrity as well as for axonal transport. Chemicals that affect axonal transport may result in axonal swelling and degeneration that is visible at the light microscopic level.

When viewed by light microscopy, large neurons are characterized by relatively large cell bodies, by nuclei with single prominent nucleoli, and by Nissl substance (Figures 1a-f). However, in small-sized interneurons and neurons such as the granule cells that are abundant in the cerebellar cortex as well as in some other brain regions such as the olfactory bulbs and cochlear nuclei, these features may not be apparent (Figures 1b-c). Interneurons (i.e., neurons having axons that remain within a particular neuroanatomic locus) are usually smaller than the projection neurons that connect with other brain regions. The striatum (caudate and putamen) is an exception to this rule, with the cholinergic interneurons being larger than the medium spiny projection neurons (Figure 1f). While the wide variation in size and appearance of neurons may be problematic for the inexperienced pathologist, it is this broad spectrum of neuron morphology that also assists in the microscopic recognition of numerous neuroanatomic regions. Recognizing these regional patterns will assist the pathologist in identifying specific brain nuclei (i.e., aggregates of neurons that perform a specific function or represent components of a particular neural pathway). Recognizing specific neuroanatomic regions and, in turn, learning the afferent and efferent connections of these regions will enhance the pathologist's understanding of pathophysiologic mechanisms within the CNS and will also make the study of neuropathology more enjoyable. For example, if neuronal degeneration is encountered within the hippocampus, the pathologist should check to see if degeneration is also present within the entorhinal cortex (which provides the primary input to the hippocampus) and should additionally check those neuroanatomic regions receiving input from the hippocampus (e.g., the subiculum, entorhinal cortex, prefrontal cortex, lateral septal area, mammillary body, and amygdala).

A variety of immunohistochemical markers exist for neurons. Some of these markers include synaptophysin, NeuN, neurofilament protein, neuron-specific enolase (NSE) (which is not entirely specific for neurons), and microtubule-associated protein 2 (MAP2). Stains for calcium-binding proteins (e.g., calbindin, parvalbumin, and calretinin) are useful in identifying some neuronal subtypes. Sections of the CNS are particularly prone to histologic artifacts that may be misinterpreted as lesions or may mask underlying neuropathologic processes. Investigators inexperienced in neuropathology have frequently published papers in which photomicrographs show artifactual dark neurons that are claimed to represent dead or even ''apoptotic'' neurons. (Note that apoptosis is not a term that should be assigned to the mechanism of cell death in the nervous system based on examination at the light microscopic level with routine stains. Use of the term ''apoptosis'' suggests that the pathologist understands the biochemical pathways leading to the cell's demise, and the morphologic features of apoptotic and nonapoptotic cell death may be similar.) Dark neurons represent the most common artifact encountered within CNS tissues and are most frequently found in brains that have been handled prior to fixation (including shortly after perfusion fixation). Although well described by Cammermyer in the 1960s (e.g., Cammermyer 1961), the significance of the dark neuron artifact seems to have been forgotten, prompting a recent review by Jortner (2006). Sometimes referred to as ''basophilic neurons,'' these dark neurons are actually amphophilic in staining character. Large-sized neurons most frequently show the dark neuron alteration, but any neuron population may be affected (Figures 2a and 2b). Nevertheless, there is a predilection for certain neuron populations to more frequently show this artifact. Examples include the pyramidal layer of the hippocampus (Figures 2a and 2c) as well as some of the major brain stem nuclei (Figure 2b). Dark neurons appear to be in a shrunken or contracted state, and it is possible that this may be the result of contraction of cytoskeletal proteins such as actin. It has recently been shown that dark neuron formation could be prevented (in cerebral cortex biopsies) by blocking glutamate receptors (Kherani and Auer 2008). Dark neurons will also be encountered in cresyl violet-stained sections (Figure 2c). However, since cresyl violet is a stain for Nissl bodies (essentially the RER), it should be recalled that disassociation of ribosomes from the RER occurs in the early stages of cell degeneration. As a result, degenerating neurons actually stain very poorly (rather than darker) with cresyl violet.

The classic appearance of neuron degeneration is that seen in the process known as ''acute eosinophilic neuron degeneration.'' The degenerating neurons (sometimes referred to as ''red dead neurons'') are characterized at the light microscopic level by cell body shrinkage, loss of Nissl substance, intensely stained eosinophilic cytoplasm, and a small/shrunken darkly stained (pyknotic) nucleus that may eventually fragment (undergo karyorrhexis) (Figures 2d-2f). The most important feature of neuron degeneration (unless peracute in nature) is that it is heterogeneous in appearance, whereas the dark neuron artifact is always monomorphic. For example, the neuropil

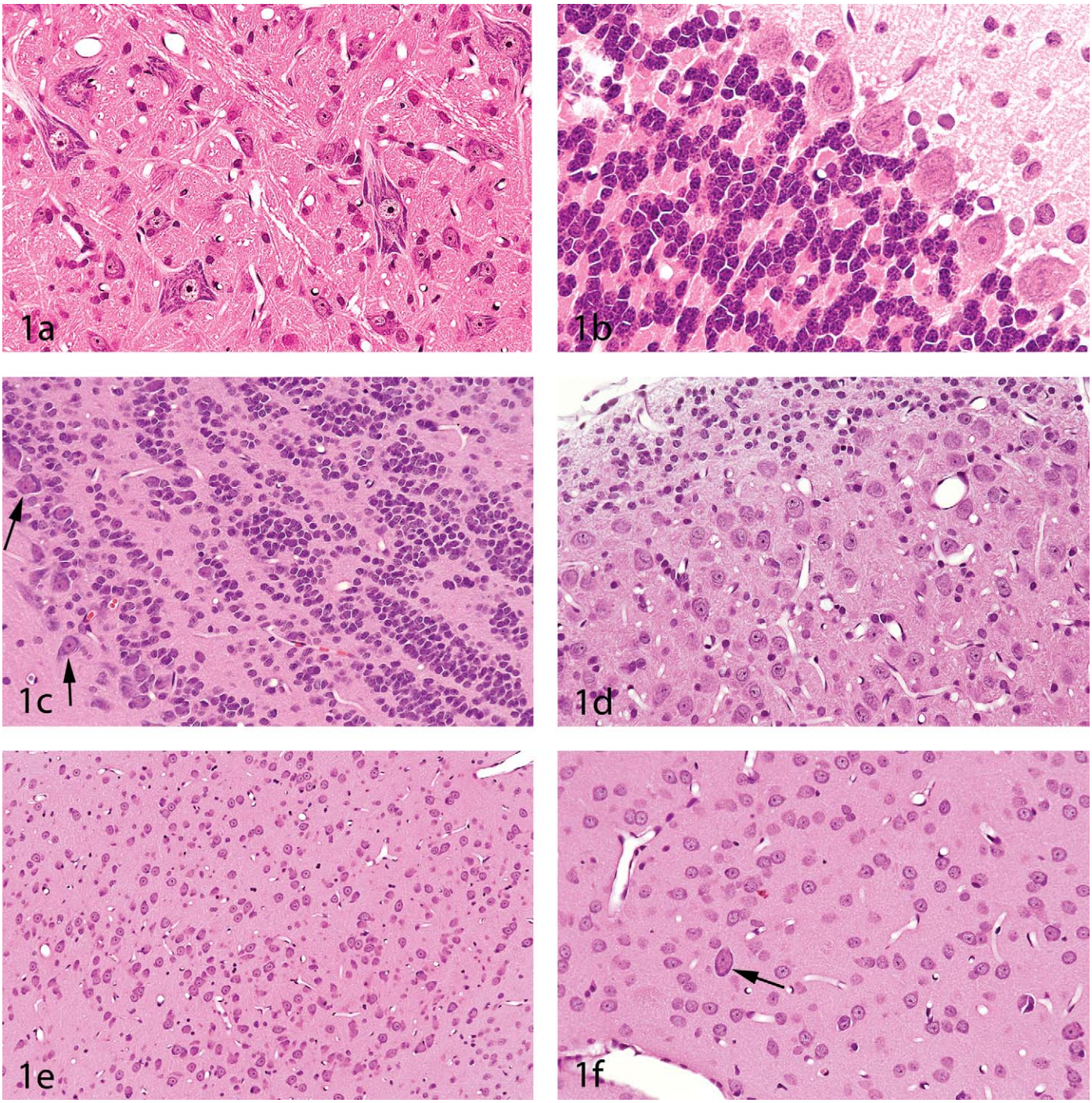

FIGURE 1.—The panels in this figure were selected to show that neuronal populations within the brain are heterogeneous. In **1a** (reticular formation), mixtures of medium- to large-sized neurons with prominent Nissl substance are present. In contrast, the cerebellum (**1b**) and olfactory bulb (**1c**) are comprised of a single layer of large-sized projection neurons (Purkinje neurons for the cerebellum and mitral cells [arrows] for the olfactory bulb) and large numbers of small-sized interneurons that are broadly classified as "granule cells." In contrast, the cochlear nucleus (**1d**) contains primarily medium- to large-sized neurons along with a "cap" of granule cells. Some brain regions such as the amygdala (**1e**) are comprised of a relatively monomorphic population of medium-sized neurons, whereas the striatum (caudate-putamen), shown in **1f**, is comprised primarily of medium-sized neurons along with scattered large-sized cholinergic interneurons (arrow). (All figures are of H&E-stained sections. Final magnifications: 1a, 1c, and 1d = 277x; 1b = 554x; 1e = 138x.)

adjacent to the degenerating neurons may be finely vacuolated as a result of swelling of neuronal processes (Figures 2d and 2e), or vacuolar alteration may be seen within the cytoplasm of neurons (Figure 2f). Furthermore, degenerating neurons will typically be found in different stages of degeneration (e.g., some having normal-appearing nuclei but eosinophilic

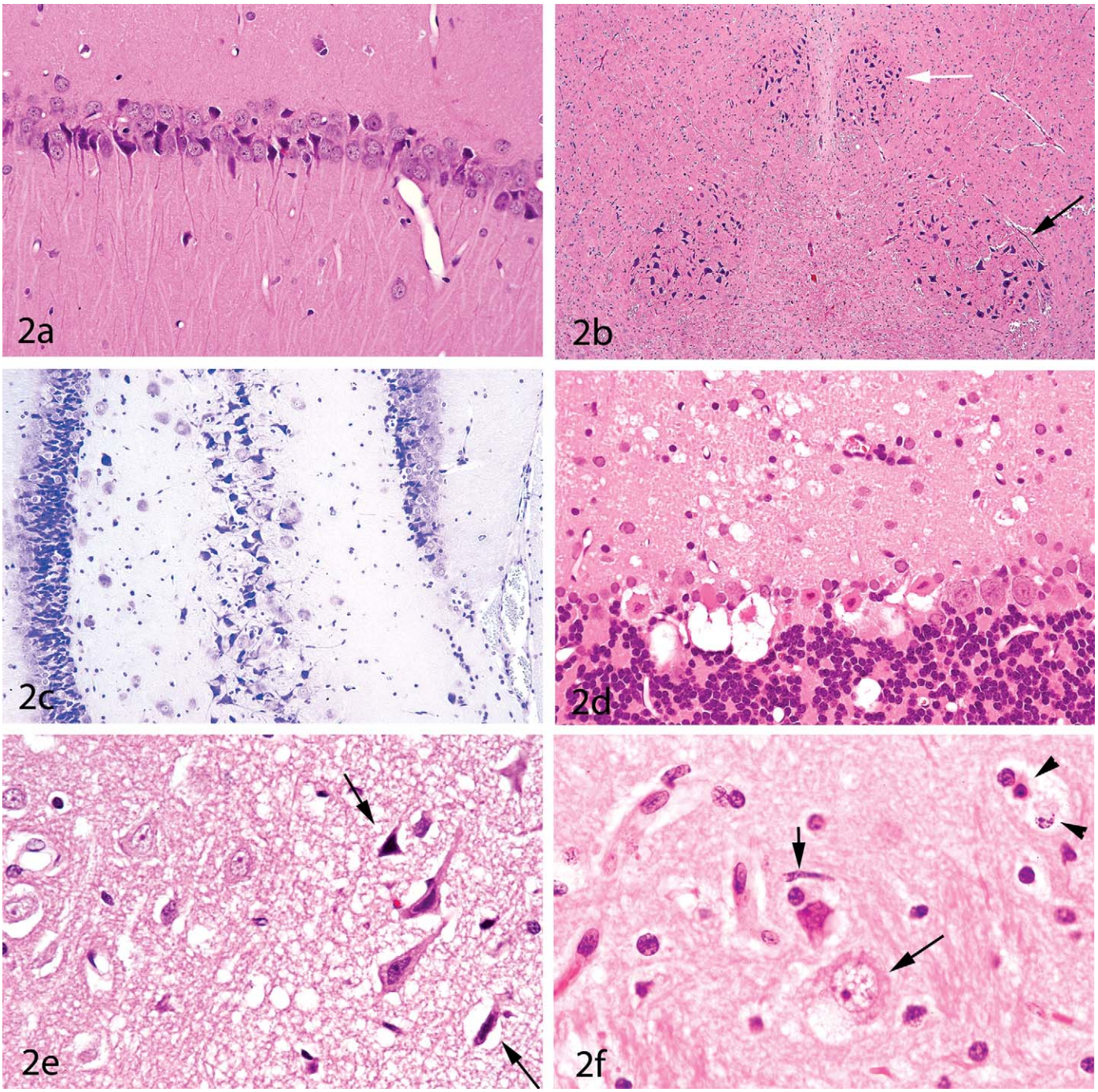

FIGURE 2.—These panels contrast neuron artifact with neuron degeneration. **2a** shows the classic monomorphic pattern of dark neurons within the pyramidal layer of the hippocampus. **2b** shows dark neurons bilaterally within two major midbrain nuclei in a rat brain (white arrow = oculomotor nucleus; black arrow = red nucleus). **2c** is a cresyl violet-stained section of the hippocampus showing dark neurons in three adjacent layers of neurons—the superior and inferior blades of the dentate gyrus (left and right sides of this micrograph, respectively) plus the intervening CA_4 pyramidal neuron layer, suggesting that pressure placed on the brain surface may have caused this change in all three layers. **2d** shows the classic appearance of eosinophilic (degenerating) Purkinje neurons with condensed nuclei and bright eosinophilic cytoplasm. In addition, there is vacuolation within the overlying molecular layer suggesting concurrent swelling/degeneration of Purkinje neuron dendrites. The section in **2e** is also characterized by neuropil vacuolation. Between the two arrows are four degenerating neurons. The two central neurons have prominent eosinophilic cytoplasm, whereas the other two are primarily characterized by nuclear pyknosis. It is this heterogeneous appearance that typifies *bone fide* neuronal degeneration. **2f** is similarly characterized by a heterogeneous pattern, including shrunken eosinophilic neurons with either pyknotic or karyorrhectic nuclei (arrowheads), neuron swelling and vacuolation (long arrow), and an active-appearing microglial cell (short arrow). (All figures other than 2c are of H&E-stained sections. Final magnifications: 2a and 2c = 277x; 2b = 55x; 1b = 554x; 2c = 138x; 2e and 2f = 554x.)

cytoplasm, whereas others have pyknotic or fragmented nuclei) (Figures 2d-2f). Unless peracute in nature, a secondary microglial response is usually also present (Figure 2f).

Special stains for degenerating neurons fall into two basic categories: silver degeneration stains such as the amino cupric silver technique (de Olmos, Beltramino, and de Olmos de Lorenzo 1994) and the Fluoro-Jade stains (B and C) (Schmued and Hopkins 2000; Schmued et al. 2005). These stains are extremely helpful for both detecting and enumerating degenerating neurons and are highly recommended for acute degenerative processes, particularly if the sections are from perfusion-fixed brains (Figures 3a-3f). (Use of these stains on sections from nonperfused brains may be problematic since red blood cells will be highlighted with both techniques.) The degeneration stains not only assist the pathologist in readily detecting medium- to large-sized degenerating neurons at lower power magnifications but also reveal degeneration within small-sized interneurons that have insufficient amounts of cytoplasm to demonstrate the eosinophilic cytoplasmic alteration typically present within H&E-stained sections. These stains are also helpful for distinguishing dark neurons from degenerating neurons within peracute degenerative processes in which the eosinophilic cytoplasmic alteration has not had time to develop (Figures 3e and 3f).

The principal advantages of the Fluoro-Jade stains include their ease of performance and that they may be used to stain sections from paraffin-embedded tissues. The silver degeneration stains, on the other hand, are more difficult to perform and are limited to sections from tissues not processed to paraffin (typically cryosectioned material). (In some safety evaluation studies, this might mean that two sets of brains would be required—one for paraffin embedding and the other for cryosectioning.) On the other hand, it is likely that silver degeneration stains would be employed only for the acute phase of a study and that paraffin-embedded tissues would be used for evaluations at later time points. Several advantages of the silver degeneration stains are that the sections can be viewed with bright field microscopy, the sections are more readily archival, and degenerative cell processes are more easily recognized. As a visual comparison of differences in staining of degenerative neuronal processes with these two techniques, Figures 3c and 3d represent two sides of the same rat brain—the left side processed to paraffin (and stained with Fluoro-Jade B) and the right side cryosectioned (and stained with amino cupric silver). It is important to note that some degrees of dendritic and axon terminal degeneration will also be revealed with the Fluoro-Jade stains even though not well illustrated in the relatively low-power images that constitute Figure 3. The bottom line is that there is no single "best stain" for detecting degenerating cells, and the stain selected (as well as the best time point for detecting a neurodegenerative process) will depend upon the dynamics of the test article and/or the experimental protocol. In some models of excitatory cell injury, the optimal sampling time point for detecting cell body degeneration will often be relatively acute (within a few days of dosing in the case of excitatory neurotoxicants), although larger sized neurons such as the pyramidal cell neurons of the hippocampus may show degenerative changes for at least two weeks (unpublished data). In this author's experience, axonal injury may also be detected (with both the Fluoro-Jade and silver degeneration stains) over a longer period of time postinjury. For example, damaged axons will be highlighted with the amino cupric silver stain for at least two weeks following traumatic brain inury (Garman, unpublished data). Furthermore, this author has found that both the silver degeneration stains and the Fluoro-Jade stains highlight the optic tracts of rats that have "unilateral optic nerve atrophy" (a degenerative condition of the optic nerves and optic tracts that is generally considered to be chronic in nature; Shibuya, Tajima, and Yamate 1993).

In addition to the degeneration stains just discussed, a number of immunohistochemical stains for proteins are important in detecting and differentiating a variety of neurodegenerative diseases (e.g., beta amyloid in Alzheimer's disease, alpha-synuclein in Parkinson's disease, tau protein in a number of neurodegenerative diseases, and prion proteins in the spongiform encephalopathies). The accumulation of intraneuronal proteins in a variety of chronic neurodegenerative diseases may be the result of increased phosphorylation or proteolysis due to the influx of calcium into stressed cells. Proteins that are designated by the cell for destruction are conjugated with a stress protein named ubiquitin, for which an immunohistochemical stain is also available. Greater detail on the use of these special stains is beyond the scope of this discussion.

ASTROCYTES

Astrocytes have multiple roles within the CNS, including maintenance of the integrity of the blood-brain barrier, uptake and recycling of glutamate and GABA, maintenance of the extracellular ionic milieu (via uptake of K^+ ions released during neuronal activity), and neuronal metabolic support. Radial astrocytes are specialized astrocytes that provide pathways for neuron migration during brain development. Within the cerebellum, some radial glia transform into the "Bergmann astrocytes" (or "Bergmann glia"), the cell bodies of which reside within the Purkinje neuron layer. Proliferation of Bergmann astrocytes—referred to as "Bergmann gliosis"—may be seen as a result of chemical toxicities that produce a loss of Purkinje neurons. Corpora amylacea, common within the brains of aging mammals (especially humans but rare in the CNS of rodents), represent glucose polymers ("polyglucosan bodies") that reside within the cytoplasm of astrocytes. Corpora amylacea are most frequently present within perivascular and subpial locations, thus corresponding to the location of astrocytic cytoplasmic processes.

Astrocytes—like neurons—have a variety of neurotransmitter receptors within their cell membranes, and astrocytes are also involved in information processing. Stimulation of astrocytes by neurotransmitters induces cell signaling (via gap junctions and involving elevations in intracellular calcium) to other astrocytes over relatively long distances (Agulhon et al. 2008). The important roles of astrocytes in supporting neuron function is underscored by the large numbers of these cells present in the

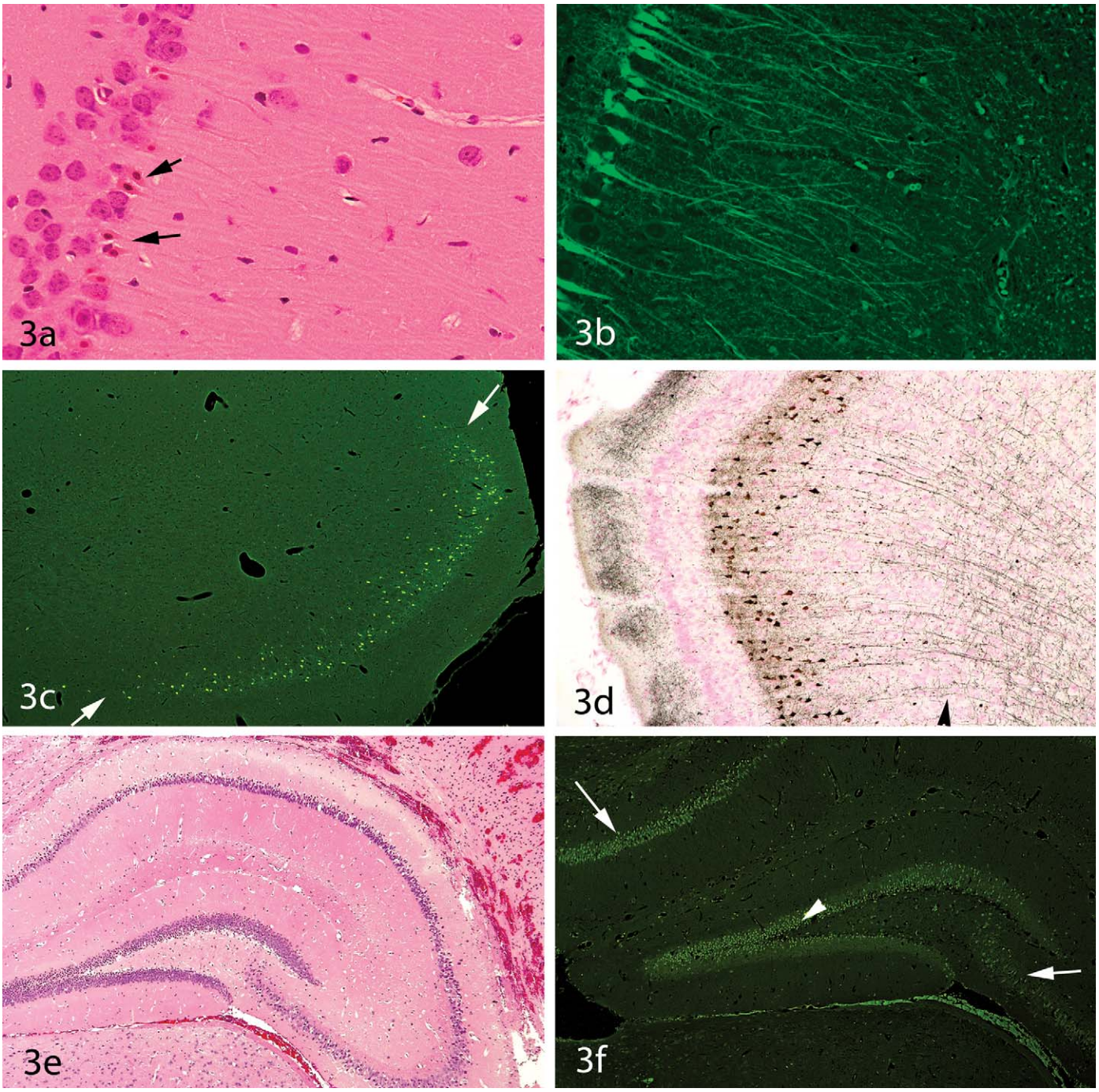

FIGURE 3.—Use of special stains to enhance detection of degenerating neurons. **3a** is of an H&E-stained section showing eosinophilic (degenerating) neurons within the pyramidal layer of the hippocampus of a rat. Arrows point to two of these degenerating neurons, but approximately nine can be visualized in this field. **3b** is an adjacent section stained with Fluoro-Jade B. Many more degenerative neurons are evident, and the neuronal processes within the stratum radiatum are also stained. **3c** and **3d** are micrographs of the retrosplenial cortex of a rat treated with MK-801. The left half of the brain was processed to paraffin and sections stained with Fluoro-Jade B (**3c**), whereas the right side of the brain was cryosectioned and stained with amino cupric silver (**3d**). In 3c, a band of yellow-stained (dead) neurons is present between the arrows. In this figure, primarily the bodies of dead cells are revealed by the Fluoro-Jade, although stained cell processes may be seen at higher magnifications. Staining of degenerative neuronal processes is easier to detect at low power magnifications with the amino cupric silver stain (e.g., the dendritic terminals in Layer 1 at left and the arrowhead pointing to degenerating axons within the underlying white matter). **3e** is a low-power micrograph of the hippocampus of a mouse that was necropsied 3 hours after the onset of status epilepticus. (Note that the hemorrhage present in the parietal cortex at the upper right was the result of a mild concussive injury.) Many dark neurons are evident that, on higher-power magnification, were difficult to differentiate from dark neuron artifact. However, a Fluoro-Jade B stain (**3f**) substantiated the degenerative nature of these dark neurons. (The arrowhead points to degenerative granule neurons in the dentate gyrus; the arrows point to degenerating pyramidal neurons in the CA_1 and CA_3 sectors.) Note that the fluorescent signal present along the interface between the hippocampus and the underlying thalamus represents autofluorescence of red blood cells within the area of congestion and hemorrhage that can be recognized in this region in **3e**. (Final magnifications: 3a and 3b = 277x; 3c = 70x; 3d = 138x; 3e = 55x; 3f = 69x.)

brain. Astrocytes are the predominant glial cell type and comprise approximately half of the volume of the adult mammalian brain (Agulhon et al. 2008). In most brain areas (and depending on the species), there is an approximately 1 to 1 ratio between the numbers of astrocytes and the number of neurons, although the ratio is higher in some brain regions and is also higher in brains from those species possessing greater cognitive abilities. For a more complete overview of astrocytic cell biology, the reader is referred to an article in this issue (Sidoryk-Wegrzynowicz et al. 2011), as well as to a recent review by Sofroniew and Vinters (2010).

To fulfill their various vital roles, astrocytes have cytoplasmic extensions that touch on the surfaces of all major regions of the neuron's anatomy (i.e., cell bodies, axons, dendrites, and synapses) and also extend to the pial surface of the brain to form the glia limitans (glial limiting membrane). The glia limitans seals the surface of the brain and also dips into the brain tissue along the perivascular (Virchow-Robin) spaces. Astrocyte foot processes also surround brain capillaries and, during development, induce endothelial cells to form tight junctions.

The term "astrocyte" means "star cell," referring to the multiple radially arranged cytoplasmic processes that can be appreciated only with special stains. However, while astrocytes have long cytoplasmic extensions that reach from neurons to the pial surface and/or to capillaries, these processes are not seen within H&E-stained sections. In fact, nonreactive astrocytes are characterized within H&E-stained sections by "naked nuclei" and little observable cytoplasm (Figure 4a). Astrocytes are often broadly classified into fibrous and protoplasmic types, with the former being found within white matter regions and the latter residing within the gray matter. This is an oversimplification, however, with newer evidence indicating that astrocyte populations are heterogeneous from one brain region to another (Yeh et al. 2009; Hewett 2009).

In gray matter regions of the CNS, astrocytic cell nuclei are often found to be in close proximity to neurons (Figure 4a) but may be found anywhere within the neuropil. Astrocyte nuclei typically have pale, finely granular chromatin patterns and relatively small or indistinct nucleoli. One of the many roles of the astrocyte is to remove and detoxify ammonia; and in states of hyperammonemia, "Alzheimer type II astrocytes" with swollen, "water clear" nuclei may be seen in sections from immersion-fixed (but not perfusion-fixed) brains (Norenberg et al. 2007) (Figure 4b).

In reactive astrocytosis, the cytoplasm of astrocytes becomes more distinct. Reactive astrocytes also have larger (i.e., more active-appearing) nuclei that are typically eccentric in position, and these cells are occasionally binucleated. Such reactive astrocytes are often referred to as "gemistocytic astrocytes" or "gemistocytes" (literally meaning "stuffed cells") (Figure 4c). The immunostain most frequently performed to demonstrate astrocytes detects the cytoskeletal protein glial fibrillary acidic protein (GFAP). Degrees of GFAP staining will vary depending upon the species, the neuroanatomic region, the method of fixation, and the antibody and staining procedure utilized. In GFAP-stained sections of normal brain tissue, the fibrous astrocytes of the white matter typically stain more prominently than do the protoplasmic astrocytes. A paucity of GFAP staining in some neuroanatomic regions (especially in formalin-fixed vs. frozen tissue) suggests that some astrocytes may have lesser concentrations or different epitopes of GFAP and/or that degrees of GFAP expression have been altered by the fixation process. Nevertheless, GFAP stains are quite useful for identifying reactive astrocytes. In GFAP-stained sections, reactive astrocytes are identified by their thickened cytoskeletal processes (Figure 4d). "Gliosis" refers to a proliferation of astrocytes within damaged regions of the CNS. However, a diagnosis of gliosis should be used with caution if increased numbers of astrocytes are encountered within H&E-stained sections in the absence of any underlying histopathologic process such as neuron loss, neuropil vacuolation, and so forth. If reactive astrocytes such as gemistocytes are present or there is prominent staining with GFAP, use of the term "gliosis" is appropriate. However, early glial cell neoplasms may be misdiagnosed as gliosis. The term "myelination gliosis" is used to describe the normal proliferation of glial cells (primarily oligodendrocytes) within the developing brain just prior to myelination.

Pathologists examining CNS sections from immersion-fixed specimens are well aware of the typical "shrinkage or fixation artifacts" that most frequently manifest as perivascular "retraction" spaces and cleft formation or vacuolation within the Purkinje cell zone or along the blades of the dentate gyrus of the hippocampus. These are regions that also happen to have abundant astrocytic cell processes. Furthermore, careful examination of these artifacts usually reveals that these spaces are not actually "clefts" but represent aggregates of vacuoles (Garman forthcoming). This author has seen at least several pharmaceutical treatments that enhanced this pattern of artifact, which, based both on location (perivascular and paraneuronal with a predilection for sites such as the Purkinje cell layer) and staining with GFAP suggested that the process was one of swelling of astrocyte cell processes immediately after death (Figures 4e and 4f). In the case of one of these pharmaceuticals, cryostat sections from snap-frozen brains did not have vacuoles, but vacuoles were prominent within paraffin sections from similarly treated animals. Of great interest to this pathologist was also the heterogeneous distribution of the vacuoles seen with these test articles. For example, in the case of the vacuolar alteration shown in Figure 4f, the globus pallidus was affected but not the caudate-putamen, once again indicating heterogeneity in astrocyte populations (or at least altered levels of astrocyte activity within the affected regions).

OLIGODENDROCYTES

Oligodendrocytes are responsible for the formation and maintenance of the myelin sheaths of the CNS. Although Schwann cells serve this role in the peripheral nervous system, oligodendrocytes will be found to extend out from the brain for some distance into the proximal segments of the cranial nerves (as well as along the entire optic nerve). Within these cranial

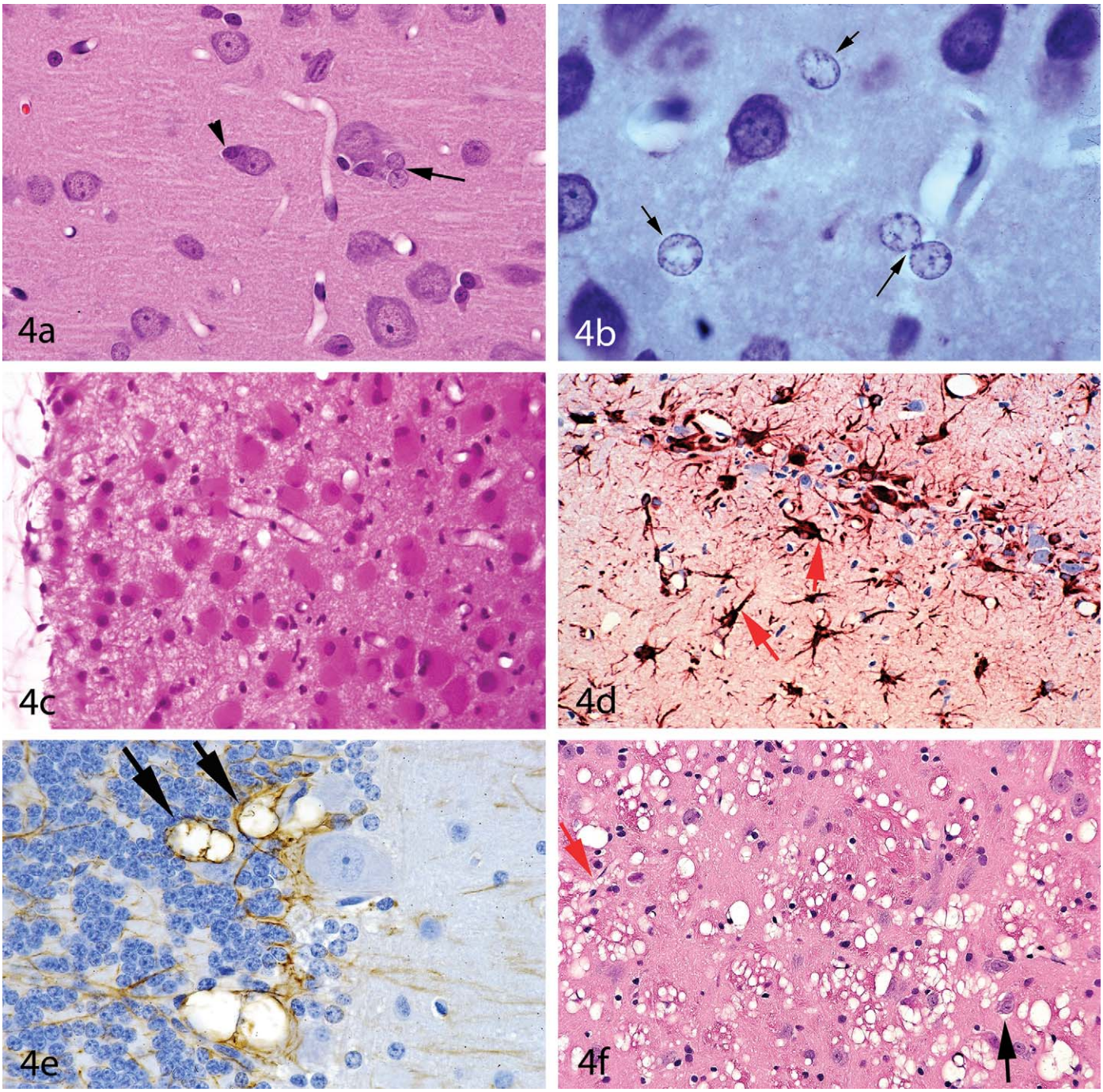

FIGURE 4.—Variations in astrocyte morphology. **4a** is a micrograph of rat cerebral cortex. The arrowhead points to a para-neuronal oligodendrocyte (often referred to as a "satellite cell"), whereas the full arrow points to two normal-appearing astrocytes. (Astrocytes are sometimes found in pairs.) Compared with oligodendrocytes, astrocytes have larger nuclei with pale vesicular chromatin patterns. Astrocytes have quite small or nonprominent nucleoli. **4b** is from the cerebral cortex of a dog with experimentally induced hyperammonemia. The astrocytes (arrows) have enlarged, relatively "clear" nuclei. These cells are referred to as Alzheimer type II astrocytes and are typically seen in hepatic encephalopathy. (Note that this image represents a copy of a borrowed film transparency, and no attempt was made to alter the color cast.) **4c** is an extreme example of astrocyte hypertrophy (primary visual cortex from a macaque monkey with chronic methyl mercury intoxication). In this field, the large cytoplasm-rich cells represent "gemistocytic astrocytes." **4d** represents a glial fibrillary acidic protein (GFAP)-immunolabeled section of rat hippocampus after loss of a large number of neurons within the CA_1 pyramidal layer. These astrocytes can be identified as being reactive/hypertrophied based upon their thick cytoskeletal processes (arrows). **4e** is a micrograph of a macaque monkey cerebellar cortex in which vacuoles were apparent in H&E-stained sections. Within this GFAP-immunolabeled section, thin rims of glial fibrillary acidic protein could be identified at the perimeter of many vacuoles, providing presumptive evidence that these vacuoles were within astrocytes. **4f** is a micrograph of the globus pallidus of a rat characterized by extensive vacuolation. Although the specific locations of these vacuoles cannot be determined at the light microscopic level, there is a tendency for the vacuoles to be adjacent to vessels (red arrow) and neurons (black arrow) but to not be within neurons. This pattern suggests that the vacuoles are within astrocytic cell processes. (All figures other than 4d and 4e are of H&E-stained sections. 4b represents a scan of a kodachrome loaned by Dr. M. D. Norenberg. Final magnifications: 4a = 554x; 4b uncertain [from a scanned kodachrome]; 4c, d, and f = 277x; 4e = 554x.)

nerves, sharp demarcations will be seen between the zones of central and peripheral myelination (Figure 5a). Oligodendrocytes—in contrast with Schwann cells—ensheath multiple axons, whereas a single Schwann cell forms the myelin sheath for only one axonal internode. Within tracts of white matter, oligodendrocytes are typically arranged in linear rows between the nerve fibers (Figure 5a). For a recent review of the biology and pathology of oligodendrocytes, the reader is referred to Bradl and Lassmann (2010).

The classic ''fried egg'' appearance of oligodendrocytes within nonperfused nervous system tissue represents cytoplasmic artifact (Figure 5b) and will not be seen in sections from perfusion-fixed brains (Figure 5c). Within the gray matter, oligodendrocytes are frequently found immediately adjacent to neuron cell bodies, where they are often referred to as ''satellite cells'' (Figure 5c). (Note that satellite cells within the sensory ganglia of the peripheral nervous system are present in large numbers but represent Schwann cells.) The term ''satellitosis'' refers to increased numbers of cells surrounding neurons. However, like ''gliosis,'' this term should be used with caution since the numbers of neuron-associated satellite cells will vary from one region of the brain to another. Neoplastic satellitosis (most frequently seen in association with malignant astrocytic neoplasms) is far more common than reactive satellitosis except in processes of neuron degeneration, within which the satellite cells represent microglia. Immunologic stains for myelin-associated glycoprotein (MAG) and for myelin basic protein (MBP) have been used to stain oligodendroglia with varying success, but the results are not always reliable or reproducible.

Myelin vacuolation or myelin sheath splitting may or may not be the result of compromised function of oligodendrocytes. Triethyltin tin, for example, produces the classic pattern of intramyelinic edema without altering the morphology of the oligodendrocyte nuclei (although some astrocytic cell swelling has been reported) (Krinke 2000) (Figure 5d). Intramyelinic edema may also be characterized by round vacuoles that are not restricted to white matter tracts (Gibson et al. 1990) (Figure 5e). Artifactual myelin vacuolation is common, and it is important that the pathologist be able to distinguish this artifact from vacuoles due to premortem alteration of the myelin sheaths. Figures 5e and 5f provide such a comparison. The vacuoles in Figures 5e and 5f are somewhat similar in that both types contain small amounts of poorly stained material. However, the vacuoles in Figure 5f (which represent artifact) are more irregular in shape. The vacuoles shown in Figure 5f—sometimes referred to as Buscaino bodies, mucocytes, or metachromatic bodies—develop as a result of handling of the brain or spinal cord too soon after exposure to formaldehyde fixatives and, in the author's experience, tend to be more prominent in tissues fixed with formalin preparations that also contain alcohol. Buscaino bodies are thought to be caused by solubilization and subsequent precipitation (by fixation) of some myelin component (Ibrahim and Levine 1967). These structures are typically pale but may be slightly basophilic or gray in color, as well as metachromatic or periodic acid-Schiff (PAS)-positive (Vinters and Kleinschmidt-DeMasters 2008). In the author's experience, Buscaino bodies are also often (but not always) refractile when viewed with polarized light.

MICROGLIA

Microglia comprise the reticuloendothelial system of the CNS and constitute 5-20% of the brain's glial cell population. As with neurons and the macroglia, microglia are functionally heterogeneous. For a concise overview of current concepts in microglial cell biology, the reader is directed to the review article in this issue (Kofler and Wiley 2011), as well as to a recent review by Graeber and Streit (2010).

In H&E-stained sections of normal brain regions, only small numbers of microglia are typically recognized. The nuclei of resting microglia are elongated or ''cigar-shaped'' and are composed primarily of heterochromatin (i.e., are darkly stained and, therefore, not active in appearance) (Figure 6a). In fact, these nuclei are sometimes mistaken for endothelial cell nuclei—or endothelial cell nuclei may be mistaken for microglia when tangential slices of capillary walls are viewed in sections from perfusion-fixed brains. (As an example of this, compare the morphology of the microglial cell indicated by the arrow in Figure 6a with the endothelial cells found adjacent to the empty vascular spaces within this same field.) The cytoplasm of nonreactive microglia is poorly visualized with routine stains. However, with special staining procedures, such as ionized calcium-binding adapter molecule 1 (Iba1), the extensive dendritic processes of microglia can be visualized (Figure 6b). Immunohistochemical markers most frequently used for microglial cells include Iba1 and lectin (*Griffonia simplicifolia*; GS-IB_4), with the CD68 (ED1) stain being helpful for revealing macrophages. A number of other immunostains have been used successfully for demonstrating microglia but will not be discussed here.

In lesions characterized by neuronal degeneration, individual microglia will typically be seen in close proximity to the degenerating neurons (Figure 2f). Greater insults to the CNS may result in denser infiltrates of microglia, some of which will assume a histiocytic cell morphology (6c) or even form granuloma-like inflammatory patterns (Figure 6d). Under appropriate conditions, microglia may transform into macrophages and, in this state, are sometimes referred to as ''gitter cells.'' In most ''neurotoxic'' lesions, neuronal degeneration will be apparent by the time microglia aggregate at the scene. However, this is not always the case. Figure 6e shows microglia surrounding a relatively normal-appearing neuron. Although this image is from an experimental lentivirus infection, this author has seen a similar pattern (i.e., of microglia surrounding normal-appearing neurons) in some toxic lesions (such as in certain stages of methylmercury intoxication). (It appears that microglia know much more about the state of health of neurons than we pathologists do with our microscopes.) After damaged neurons have been removed by activated microglia, residual microglial nodules may remain (Figure 6f).

In addition to microglial cells, other cells of mesenchymal origin (which will not be discussed here) include those within

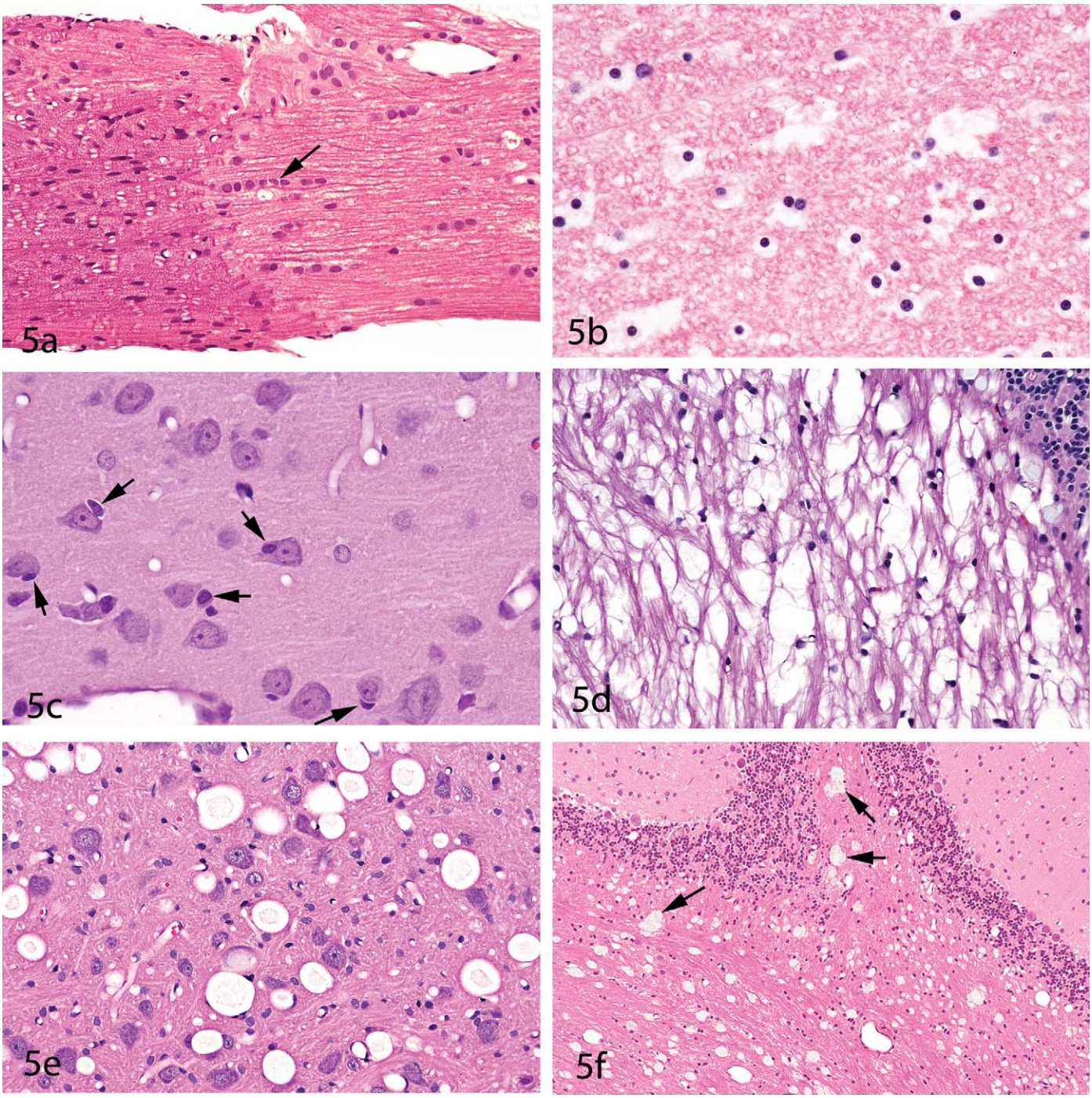

FIGURE 5.—Morphology of oligodendrocytes and selected patterns of myelin vacuolaton. **5a** is of a trigeminal nerve and shows the difference between the normal myelination pattern of the CNS (at right) and PNS (at left). Oligodendrocytes in CNS white matter tracts often line up (arrow). **5b** shows normal oligodendrocytes with prominent perinuclear haloes, producing the typical "fried egg" appearance of these cells in immersion-fixed material (micrograph of an immersion-fixed dog brain). Such haloes are not seen in perfusion-fixed material. In **5c** (cerebral cortex from a rat), arrows point to 5 oligodendrocytes. These cells have small, round, relatively dark nuclei and, within the gray matter regions of the brain, are often in close proximity to neurons (thus being referred to as "satellite cells"). **5d** shows extensive myelin vacuolation within the cerebellar white matter of a rat (due to triethyltin toxicity). However, the oligodendrocyte nuclei are microscopically normal. These vacuolar clefts are typically empty and represent the classic pattern of "myelin sheath splitting." Although the vacuoles in **5e** (present within one of the deep cerebellar nuclei of a rat) differ in morphology from the myelin clefts shown in 5d, ultrastructural evaluations revealed that these vacuoles also represented myelin sheath splitting. Note that some of these vacuoles contain small amounts of poorly stained material. The vacuoles in 5e must be differentiated from myelin artifact of the type shown in **5f**. These "vacuoles" also contain some poorly stained material and often demonstrate partial birefringence when viewed with polarized light. These artifacts are most frequently seen in brains handled too soon after perfusion fixation with formalin preparations containing alcohol and are sometimes referred to as Buscaino bodies or mucocytes. Note that these "vacuoles" (actually deposits) are less regular in configuration than those in 5e. (All Figure 5 panels are of H&E-stained sections. Final magnifications: 5a-5c = 554x; 5d & 5e = 277x; 5f = 138x.)

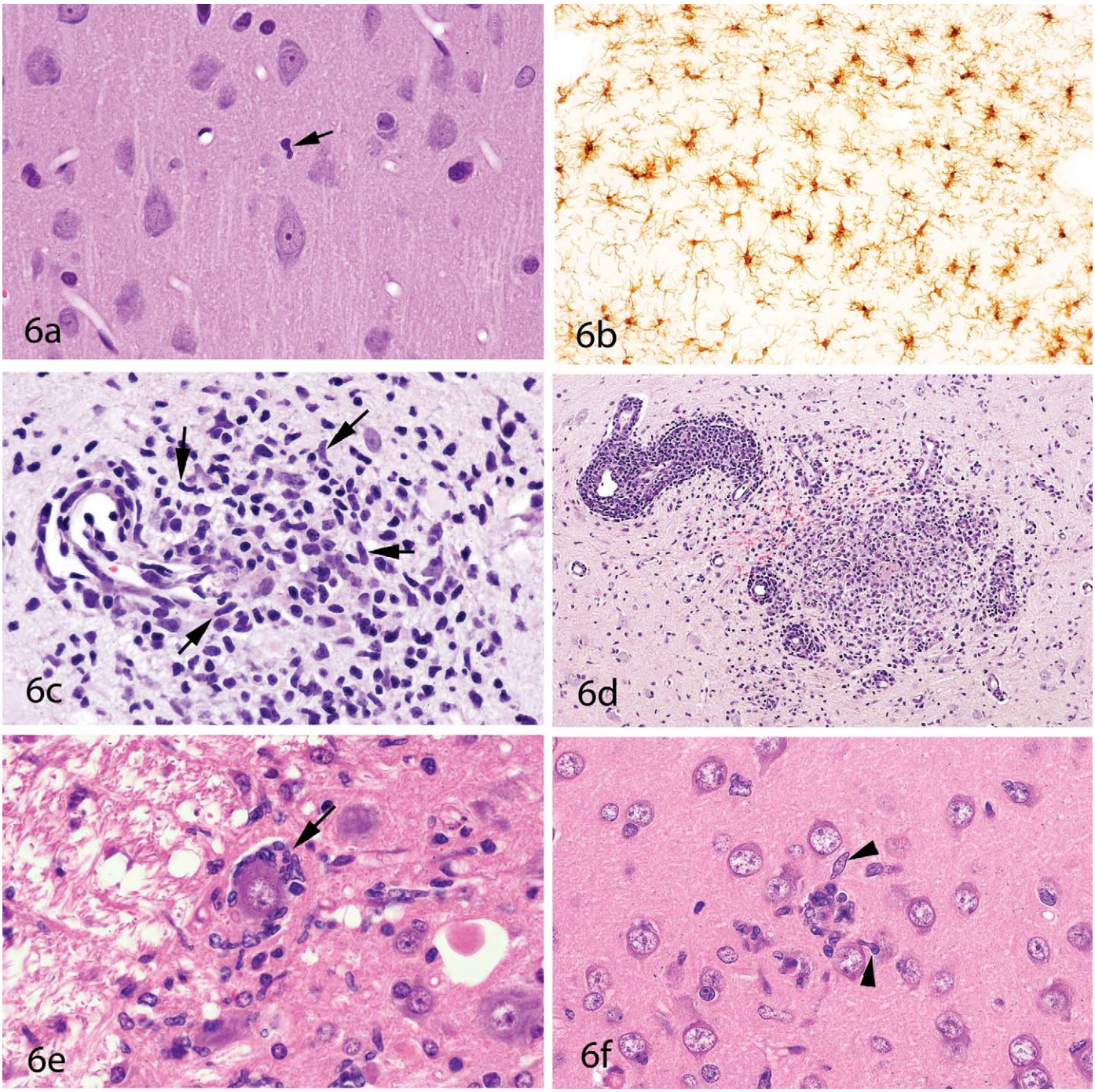

FIGURE 6.—Microglial cell morphology. Within the normal neuropil (**6a**), microglial cell nuclei are observed in relatively small numbers (arrow). These nuclei are rod-shaped and often irregularly contoured. In sections stained with ionized calcium-binding adaptor molecule 1 (Iba1) (**6b**), many more microglia will be visualized, as will their complex cytoplasmic dendritic patterns. Within inflammatory foci in the CNS, typical rod-shaped microglia (arrows in **6c**) will often be found together with other mononuclear cells such as histiocytes (possibly representing activated/transformed microglia). Well-circumscribed foci of mononuclear inflammation coupled with lymphoid infiltrates may take on a ''granulomatous'' morphology (**6d**). Microglia may be found in association with eosinophilic neurons. However, in viral infections of the CNS, microglia may be found surrounding relatively normal-appearing neurons (**6e**, arrow). As the neurons degenerate, residual ''microglial nodules'' may be all that remain of the degenerative process (**6f**, arrowheads pointing to two microglial cells). (All Figure 6 panels other than 6b are of H&E-stained sections. Panels 6e and 6f were prepared from a slide loaned by Dr. J. Ward. Final magnifications: 6a, c, e, and f = 554x; 6b and 6d = 277x.)

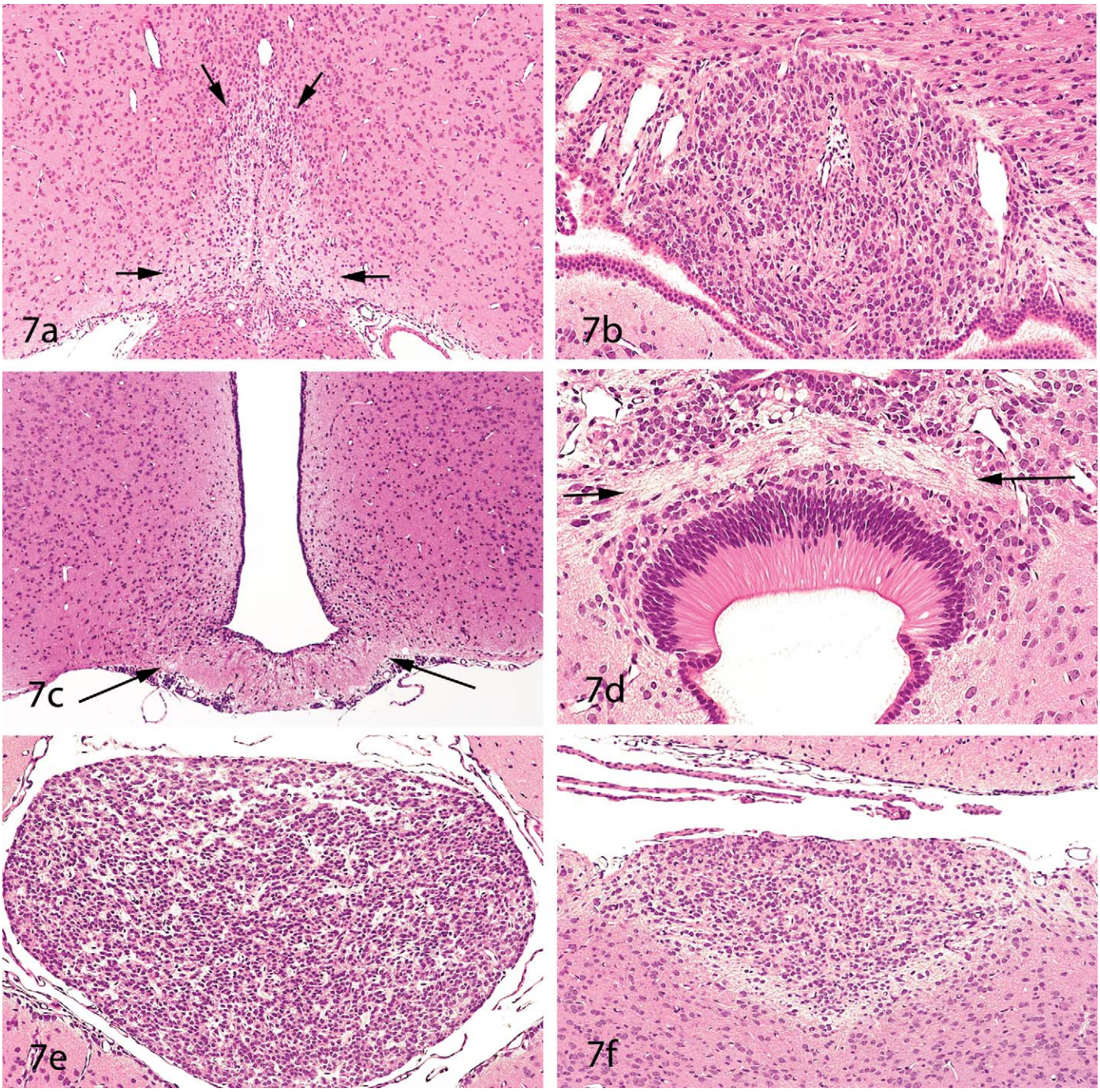

FIGURE 7.—Circumventricular organs (CVOs). These six brain regions are characterized by incomplete blood-brain barriers and have a heterogeneous appearance in rat brains. They include the organum vasculosum of the lamina terminalis (**7a**), subfornical organ (**7b**), median eminence (**7c**), subcommissural organ (**7d**), pineal (**7e**), and area postrema (**7f**). Only the CVOs in 7a, b, and f contain neurons. The subfornical organ (7b) is occasionally mistaken for a lesion (e.g., as a subependymal granuloma). The posterior commissure (arrows in 7d) appears hypomyelinated, because this image was taken from the brain of a rat pup at postnatal day 21 (an age when myelination is not complete). (All Figure 7 panels are of H&E-stained sections. Final magnifications: 7a, c, and d = 55x; 7b, e, and f = 138x.) Note that all micrographs are of rat brains.

the meninges (dura mater, pia mater, and arachnoid). Adipose tissue is occasionally seen within the choroid plexus and filum terminale regions, and fat cells within the CNS uncommonly form lipomas.

CIRCUMVENTRICULAR ORGANS

A number of specialized structures are present along the midline of the ventricular system of the brain. These are collectively referred to as the "circumventricular organs" (CVOs).

TABLE 1.—Names and locations of the circumventricular organs (CVOs).

Figure	Name of CVO	Location
7a	Vascular organ (organum vasculosum) of the lamina terminalis	Located above the optic chiasm at the rostral (anterior) limit (lamina terminalis) of the ventral floor of the third ventricle
7b	Subfornical organ	Located just beneath the fornix of the hippocampus (projecting downward into the rostro-dorsal portion of the third ventricle)
7c	Median eminence	Located at the floor of the ventral (inferior) portion of the third ventricle
7d	Subcommissural organ	Located just inferior to the posterior commissure, which is present near the opening of the mesencephalic aqueduct (of Sylvius)
7e	Pineal gland	Dorsal (superior) and/or caudal (posterior) to the third ventricle, just above the superior surface of the posterior thalamus or midbrain
7f	Area postrema	Located at the caudal (posterior) lip of the fourth ventricle adjacent to the opening of the spinal canal

Generally, six CVOs are recognized in mammals, although one of these (the subcommissural organ) is vestigial in the adult human brain. It is important for pathologists to know the locations and appearances of these CVOs since they are frequently not present within standard coronal sections and, therefore, have often been mistaken for neoplasms or other lesions. The names of the CVOs and their locations, along with the corresponding panel number in Figure 7, are listed in Table 1. These CVOs are all located on the midline. However, some neuroscientists consider the choroid plexus (with multiple locations) to represent a seventh CVO. Another region that is sometimes included in the list of CVOs is the neurohypophysis, which functions to secrete oxytocin and vasopressin into the blood.

Although the locations of the CVOs are listed in Table 1, it is recommended that the reader also check standard atlases of neuroanatomy for visual confirmation of their specific neuroanatomic locations. A good reference on the comparative anatomy and vascularization of the CVOs is that of Duvernoy and Risold (2007).

Only three of the CVOs—the organum vasculosum, the subfornical organ, and the area postrema—contain neurons. The pineal gland is composed of glia and pinealocytes but contains no true neurons. (Pinealocytes synthesize melatonin from serotonin and also contain norepinephrine and thyrotropin-releasing hormone.) The subcommissural organ consists entirely of specialized ependymal cells. The median eminence is of low cellularity, representing the site where neurohormones from various hypothalamic nuclei are released into the hypothalamo-hypophysial vasculature. CVOs function to regulate biologic rhythms (pineal gland), blood pressure and water balance (organum vasculosum, subfornical organ, and area postrema), food aversions (area postrema), and homeostasis (median eminence and pineal gland). The functions of the subcommissural organ are poorly understood, but it is known that this CVO secretes a variety of glycoproteins into the cerebrospinal fluid, some of which aggregate to form the Reissner's fiber that extends caudally through the aqueduct and spinal canal (Vio et al. 2008). The ability of the CVOs to perform their functions relates, in part, to the fact that their capillaries have fenestrated endothelial linings (i.e., lack the "tight junctions" of most of the capillaries within the CNS), and they, therefore, lack a blood-brain barrier. The lack of a blood-brain barrier within these CVOs indicates that they potentially represent important points of entry of chemicals into the brain. Therefore, when histology-based tracing studies are performed (e.g., to show the distribution of chemicals into the brain), it is essential that the CVOs be sampled. It is important to note here that certain other brain regions also lack blood-brain barriers. One example is the arcuate nucleus (which is just rostral to the median eminence and closely associated with it); another is the nucleus of the solitary tract (which is in close proximity to the area postrema). It has been suggested that these latter regions are important in regulation of food intake (Orlando et al. 2005). It follows that these regions should also sampled when looking for points of entry of chemicals into the brain.

CONCLUDING REMARKS

It is hoped that the images in this article will assist pathologists in becoming more familiar with the cytologic appearances of cells in the CNS and of the histologic patterns that characterize selected neuroanatomic regions. The reader is encouraged to embark on a journey of gradually acquiring increased knowledge of neuroanatomy and of current concepts in the neurosciences. When beginning this journey, it is helpful to have a good brain atlas at hand (for the species being examined) and to try to find a new anatomic location within each brain examined. The pathologist will find that knowledge of neuroanatomy—and subsequently of neurophysiology and neurochemistry—will make neuropathologic evaluations more exciting and more rewarding. As knowledge of neuroanatomy and of brain complexity are acquired, pathologists will also come to understand why more rigorous sampling of the CNS is being recommended for microscopic assessment in safety evaluation studies (Hale et al. 2011 [this issue]).

REFERENCES

Agulhon, C., Petravicz, J., McMullen, A. B., Sweger, E. J., Minton, S. K., Taves, S. R., Casper, K. B., Fiacco, T. A., and McCarthy, K. D. (2008). What is the role of astrocyte calcium in neurophysiology? *Neuron* **59**, 932–46.

Bolon, B., Bradley, A., Garman, R. H., and Krinke, G. J. (2011). Useful toxicologic neuropathology references for pathologists and toxicologists. *Toxicol Pathol* **39**, 234–239.

Bradl, M., and Lassmann, H. (2010). Oligodendrocytes: biology and pathology. *Acta Neuropathol* **119**, 37–53.

Cammermeyer, J. (1961). The importance of avoiding "dark" neurons in experimental neuropathology. *Acta Neuropathol* **1**, 245–70.

de Olmos, J. S., Beltramino, C. A., and de Olmos de Lorenzo S. (1994). Use of an amino-cupric-silver technique for the detection of early and semiacute neuronal degeneration caused by neurotoxicants, hypoxia, and physical trauma. *Neurotoxicol Teratol* **16**, 545–61.

Duvernoy, H. M., and Risold, P.-Y. (2007). The circumventricular organs: an atlas of comparative anatomy and vascularization. *Brain Research Reviews* **56**, 119–47.

Garman, R. H. (forthcoming). Common histologic artifacts in nervous system tissues. In Fundamental Neuropathology for Pathologists and Toxicologists: Principles and Techniques (B. Bolon and M. Butt, eds.). John Wiley, New York, NY.

Gibson, J. P., Yarrington, J. T., Loudy, D. E., Gerbig, C. G., Hurst, G. H., and Newberne, J. W. (1990). Chronic toxicity studies with vigabatrin, a GABA-transaminase inhibitor. *Toxicol Pathol* **18**, 225–38.

Graeber, M. B., and Streit, W. J. (2010). Microglia: biology and pathology. *Acta Neuropathol* **119**, 89–105.

Hale, S. H., Andrews-Jones, L., Jordan, W. H., Jortner, B. S., Boyce, R. W., Boyce, J. T., Switzer, R. C., III, Butt, M. T., Garman, R. H., Jensen, K., Krinke, G., and Little, P. B. (2011). modern pathology methods for neural investigations. *Toxicol Pathol* **39**, 52–57.

Hewett, J. A. (2009). Determinants of regional and local diversity within the astroglial lineage of the normal central nervous system. *J Neurochem* **110**, 1717–36.

Ibrahim, M. Z. W., and Levine, S. (1967). Effect of cyanide intoxication on the metachromatic material found in the central nervous system. *J Neurol Neurosurg Psychiat* **30**, 545–55.

Jortner, B. S. (2006). The return of the dark neuron. A histologic artifact complicating contemporary neurotoxicologic evaluation. *NeuroToxicology* **27**, 628–34.

Kherani, Z. S., and Auer, R. N. (2008). Pharmacologic analysis of the mechanism of dark neuron production in cerebral cortex. *Acta Neuropathol* **116**, 447–52.

Kofler, J., and Wiley, C. A. (2011). Microglia: key innate immune cells of the brain. *Toxicol Pathol* **39**, 103–114.

Krinke, G. J. (2000). Triethyl tin. In Experimental and Clinical Neurotoxicology (P. S. Spencer and H. H. Schaumburg, eds.), p. 1206. Oxford University Press, New York, NY.

Norenberg, M. D., Jayakumar, A. R., Rama Rao, K. V., and Panickar, K. S. (2007). New concepts in the mechanism of ammonia-induced astrocyte swelling. *Metab Brain Dis* **22**, 219–34.

Orlando, F. A., Goncalves, C. G., George, Z. M., Halverson, J. D., Cunningham, P. R., and Meguid, M. M. (2005). Neurohormonal pathways regulating food intake and changes after Roux-en-Y gastric bypass. *SOARD* **1**, 486–95.

Schmued, L. C., and Hopkins, K. J. (2000). Fluoro-Jade B: a high affinity fluorescent marker for the localization of neuronal degeneration. *Brain Res* **874**, 123–30.

Schmued, L. C., Stowers, C. C., Scallet, A. C., and Xu, L. (2005). Fluoro-Jade C results in ultra high resolution and contrast labeling of degenerating neurons. *Brain Res* **1035**, 24–31.

Shibuya, K., Tajima, M., and Yamate, J. (1993). Unilateral atrophy of the optic nerve associated with retrograde and anterograde degenerations in the visual pathways in Slc:Wistar rats. *J Vet Med Sci* **55**, 905–12.

Sidoryk-Wegrzynowicz, M., Wegrzynowicz, M., Lee, E., Bowman, A. B., and Aschner, M. (2011). Role of astrocytes in brain function and disease. *Toxicol Pathol* **39**, 115–123.

Sofroniew, M. V., and Vinters, H. V. (2010). Astrocytes: biology and pathology. *Acta Neuropathol* **119**, 7–35.

Vinters, H. V., and Kleinschmidt-DeMasters, B. K. (2008). General pathology of the central nervous system. Chapter 1 in Greenfield's Neuropathology (S. Love, D. N. Louis, and W. Ellison, eds.), 8th Edition, Chapter 1, pp. 1–62. Edward Arnold, London.

Vio, K., Rodriguez, S., Yulis, C. R., Oliver, C., and Rodriguez, E. M. (2008). The subcommissureal organ of the rat secretes Reissner's fiber glycoproteins and CSF-soluble proteins reaching the internal and external CSF compartments. *Cerebrospinal Fluid Res* **5**, 3.

Yeh, T., Lee, D. Y., Gianino, S. M., and Gurmann, D. H. (2009). Microarray analyses reveal regional astrocyte heterogeneity with implications for neurofibromatosis type 1 (NF1)-regulated glial proliferation. *Glia* **57**, 1239–49.